Particulates, unregulated and regulated emissions and catalytic converter efficiency evaluation of methanol (M15) fuelled BS-VI compliant light-duty spark-ignition engine

Ankur Kalwar [a], Rahul Kumar Singh [a], Ankit Gupta [b], Ranjeet Rajak [b], Gokul Gosakan [b], Avinash Kumar Agarwal [a,*]

[a] *Engine Research Laboratory, Department of Mechanical Engineering, Indian Institute of Technology Kanpur, Kanpur 208016, India*
[b] *Maruti Suzuki India Limited, Manesar, Gurugram 122051, India*

HIGHLIGHTS

- Use of M15 in BS-VI 2020 compliant light-duty MPFI SI engine was explored.
- Catalytic conversion efficiency for regulated/unregulated emissions was assessed.
- Reductions in CO, HC and PM emissions from M15 fueled engine were observed.
- NOx emissions from M15 were comparable to gasoline-fueled engine.
- Lower benzene & toluene but higher methanol/ethane emissions observed from M15.

GRAPHICAL ABSTRACT
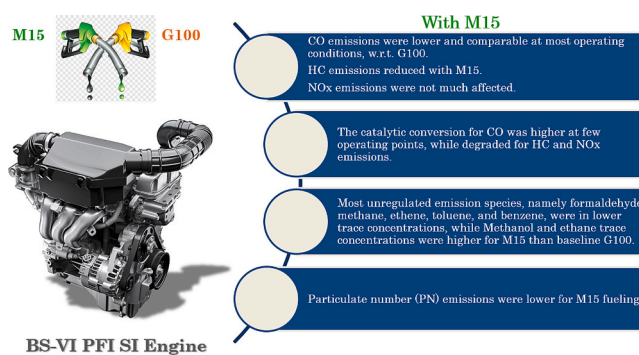
ARTICLE INFO

ABSTRACT

Methanol adaptation in the transport sector is being encouraged worldwide. Methanol, a high-octane fuel, is emerging as a strong fuel candidate for powering spark-ignition (SI) engines and it can be indigenously produced from low-value agricultural biomass waste and high-ash coal. This study investigated particulates and unregulated and regulated emissions from M15 (15 % v/v methanol, 82 % v/v gasoline, 3 % v/v propanol) fueled Bharat Stage-VI (BS-VI) 2020 compliant light-duty SI engine equipped with a multipoint port fuel injection system and compared it with baseline gasoline fueled engine. The catalytic conversion efficiency for controlling regulated and unregulated emission species are also discussed for both test fuels. The experimental results showed a reduction in carbonaceous emissions from M15 fueled engine. Hydrocarbons (HC), carbon monoxide (CO) and particulate emissions reduced, while oxides of nitrogen (NOx) emissions were comparable to baseline gasoline-fueled engine. The catalytic conversion of CO emission was higher for M15 but lower for HC and NOx emissions. Various unregulated trace emission components such as formaldehyde, acetaldehyde, methane, ethene and propene reduced with methanol addition to gasoline. Considerable reductions in benzene and toluene trace emissions were observed for M15, but methanol and ethane trace emissions were higher. The catalytic conversion of all unregulated trace emission components was comparable for both test fuels except alcohols, where

M15 exhibited increased trace emission values. The study reflected that M15 could easily replace gasoline in BS-VI-compliant light-duty SI transportation engines. However, verification of all regulatory emission compliances, diagnostics and durability compliances need be ascertained before large-scale implemetation.

1. Introduction

Introduction of alternate fuels is one of the most important internal combustion (IC) engine transformations in the historical evolution of the transport sector. Alternate fuels have the potential to make the engines cleaner, environment-friendly, sustainable, and more efficient. It also safeguards energy security since global crude oil reserves are finite and limited to specific geographical regions. Hence, policymakers plan to introduce an alternate fuel energy mix in the transport sector, which includes primary alcohols (ethanol, methanol, butanol), biodiesel, hydrogen, compressed natural gas (CNG), dimethyl ether (DME), etc. (Bae and Kim, 2017; Singh et al., 2021). Primary alcohols such as methanol and ethanol are produced from low-value biomass resources, making their production more sustainable. Most countries have already started ethanol blending programs (EBP) for gasoline in the transport sector. In India, 10 % v/v ethanol-blended gasoline (E10) is already used, and the blending level is expected to reach 20 % v/v ethanol in gasoline (E20) by 2025. In addition to ethanol, the government is also pushing the Methanol blending program (MBP) under the aegis of the National Institution for Transforming India (NITI) Ayog, in which methanol blended gasoline (M15) is being considered as a fueling option after evaluating its technical feasibility. China is already using methanol-gasoline blends extensively in its transport sector. Methanol has most favourable fuel properties among primary alcohols, such as the lowest carbon (w/w) content, the highest oxygen (w/w) content and a very high octane rating. These properties enhance the SI engine efficiency and performance of methanol-gasoline blends (Agarwal et al., 2021). However, evaluating the emission characteristics of these biofuel-powered engines is equally important since they are also required to satisfy prevailing emission norms and comply with future emission norms, in order to improve ambient air quality and reduce adverse health impacts of engine-out pollutants and climate effects.

Research studies have investigated the effect of methanol-gasoline blends on SI engine emission characteristics. Liu et al. (Liu et al., 2007) reported that port-fueled SI engines could be operated with lower methanol blends (up to 30 %) without any hardware modifications. They reported lower HC and CO emissions, and the three-way catalytic converter (TWC) conversion was efficient without any noticeable adverse effect. The study by Arapatsakos et al. (Arapatsakos et al., 2003), Balki et al. (Balki et al., 2021) and Agarwal et al. (Agarwal et al., 2014) also supported these observations. However, HC emissions were higher or lower for methanol-gasoline blends, depending on the engine's operating conditions (Agarwal et al., 2014). Similarly, some studies found that NOx emissions increased with methanol blending of gasoline (Shayan et al., 2011; Ni et al., 2014). A lower fraction of methanol did not influence the in-cylinder charge temperature due to its evaporation; hence during the high-temperature combustion, its fuel-bound oxygen enhanced the oxidation of atmospheric nitrogen. However, NOx emissions were generally reduced for blends with higher methanol fractions, such as 85 % v/v methanol in gasoline (M85) (Yanju et al., 2008). Some studies have shown that methanol-gasoline blend fueling deteriorated the engine's cold-start capabilities due to lower volatility of methanol (Gardiner et al., 1990). However, the conclusions vary due to differences in fuel blending ratios, engine designs and experimental conditions. In a study by Hu et al., the researchers claimed improved cold-start with up to 30 % v/v methanol blending of gasoline (Hu et al., 2007). As a consequence, the unburnt HC and CO emissions during cold-start reduced significantly for methanol-gasoline blends. The charge cooling differences in lower methanol-gasoline blends might not be significant, hence it did not deteriorate combustion. The benefits of lower emissions

from methanol blends were also explored in a direct injection spark ignition (DISI) engine (Feng et al., 2020). Methanol-gasoline blends were also experimentally evaluated by converting a CI engine into an SI engine. In a similar attempt, Prasad et al. (Prasad et al., 2020) studied the effect of a higher Methanol blending ratio (M50) in a higher compression ratio (CR: 10) engine. They reported a reduction in CO, HC and NOx emissions by 30–40 % vis-à-vis baseline gasoline. In another study (Güdden et al., 2021), methanol combustion's benefits were achieved in a spark-ignited modified large-bore engine (Originally a CI engine). Studies involving 100 % methanol use in SI engines showed lower emissions. Wu et al. (Wu et al., 2016) compared the engine performance of gasoline and methanol in lean-burn conditions. The ignition timings were set for each condition's highest indicated thermal efficiency. Besides higher indicated thermal efficiency from methanol combustion, HC and CO emissions were also lower. Improved charge homogeneity and a higher degree of completion of combustion were reported to be the reasons for these trends. Also, due to its lower adiabatic flame temperature, 100 % methanol combustion significantly reduced NOx formation. Celik et al. (Celik et al., 2011) explored methanol combustion with similar and higher compression ratios. The engine operated smoothly with a compression ratio of 10 when fueled with methanol, and it exhibited knocking with a compression ratio of >8 when fueled with gasoline. They found reduced CO, CO_2 and NO_x emissions but increased HC emissions with Methanol fueling. A lower peak combustion temperature led to engine misfire and partial burns, producing higher HC emissions.

From these studies, it can be inferred that methanol blending of gasoline and optimisation of engine control parameters for a specific blend can control most of the regulated emission components. However, several other harmful pollutant species exist in engine exhaust in insignificant or trace quanties, and the emission legislations do not regulate them. But these unregulated emission species may have serious adverse health impacts upon prolonged exposure. Therefore, these unregulated species must be experimentally evaluated before implementing any new alternative fuel on a large-scale. Different unregulated emission species, such as aldehydes, carboxylic acids, alkanes, alkenes, alcohols, aromatic compounds, ammonia, sulfur oxides, etc., were detected using experimental techniques, such as Fourier transform infrared (FTIR) and gas chromatography (GC) (Geng et al., 2015a). Few studies also investigated unregulated emissions from methanol-gasoline blend-fueled SI engines. Agarwal et al. (Agarwal et al., 2015) analysed unregulated emissions from lower ethanol-gasoline and methanol-gasoline blends (gasohols) fueled SI engine powering a passenger vehicle. They reported that gasoline fueling emitted higher traces of alkanes and alkenes, formic acid and benzene, than gasohols. On the other hand, methanol-gasoline blends emitted higher traces of methanol, formaldehyde and toluene in the engine exhaust than baseline gasoline. Studies by Shengua et al. (Liu et al., 2007), Wei et al. (Wei et al., 2009) and Ni et al. (Ni et al., 2014) also reported higher trace emissions of unburnt methanol and formaldehyde due to methanol blending of gasoline. TWC light-off temperature influences the tail-pipe emissions from an engine. Methanol emissions almost disappeared from the engine exhaust once the light-off temperature of the TWC (270 °C) was attained. However, formaldehyde emissions increased downstream of the TWC (Wei et al., 2009). ITO et al. (Ito et al., 1982) claimed that formaldehyde emissions increased for methanol-gasoline blend fueling due to the oxidation of unburnt methanol after combustion. Singh et al. (Singh et al., 2022a) reported that the methanol-gasoline blend (M10) was more effective among other ethanol and butanol-based gasohols in reducing unregulated trace emissions such as sulfur dioxide, ammonia,

and various other saturated and unsaturated hydrocarbons namely acetylene (C_2H_2), ethylene (C_2H_4), and propene (C_3H_6).

Regarding particulate emissions in the Euro-VI emission legislations, only gasoline direct injection (GDI) engines are covered among the SI engines. The particulate mass (PM) limit of 0.005 g/km and particulate number (PN) limit of 6×10^{11} #/km are applicable for both gasoline and diesel engines, which is evaluated using the new European driving cycle (NEDC). Studies indicated that PFI SI engines emit more nanoparticles; hence, technologies for reducing particulate emissions need to be developed, considering evolving emission legislations, which will become stricter with time unidirectionally (Price et al., 2006). Liang et al. (Liang et al., 2013) compared particulate emissions from GDI and PFI engine-powered vehicles fueled by M15 and baseline gasoline in the NEDC. The PFI engine-powered vehicle exhibited lower PM and PN emissions than the GDI engine-powered vehicle. M15 further reduced particulate emissions in both PFI and GDI engine-powered vehicles. Several studies indicated the advantages of primary alcohols in reducing particulate emissions from SI engines due to fuel-bound oxygen (Storey et al., 2012; Kalwar et al., 2020). Agarwal et al. (Agarwal et al., 2014) reported reduced PN and PM emissions by adding up to 20 % *v/v* methanol in gasoline. Singh et al. (Singh et al., 2022b) also reported that M10 fueling reduced the particulate emissions at medium-to-high loads. However, a higher alcohol blending might not lead to a favourable trend. Geng et al. (Geng et al., 2015b) reported lower PM emissions from M15, but PM emissions increased for M45 fueling. The literature review shows the emission benefits of methanol usage in engines. Since policymakers plan to introduce MBP on a commercial scale globally and, more specifically, in India, it becomes necessary to investigate its effect on current BS-VI-compliant SI engines used in the transport sector. BS-VI emission norms correspond to Euro-VI emission legislations adopted worldwide, with slight differences in driving cycles customised to Indian conditions. Hence, in this study, comprehensive emission characterisation of M15 fueling vis-à-vis baseline gasoline (G100) fueling was done in a light-duty, preconfigured, commercial, BS-VI complaint, PFI technology equipped, SI engine used in small cars in India. PFI engines using a high compression ratio complying with Euro-VI emission legislations are rarely investigated, which makes this study quite novel. Another novel aspect of this study is that it investigated the effectiveness of the TWC in controlling the regulated and unregulated emission species for both test fuels.

2. Experimental setup and methodology

The experiments for this study were performed on the 3-cylinder, port-fuel-injected, BS-VI 2020 compliant, multipoint port fuel injection (MPFI), light-duty, SI engine of a popular Indian passenger car. Detailed specifications of the test engine are given in Table 1. The steady-state testing of the engine was done on an eddy current dynamometer (Dynalec; ECB50–200), which controlled the engine load and speed.

The test setup was equipped with various instruments such as thermocouples, controllers, and pressure gauges to measure the coolant temperature before and after the radiator, lubricating oil temperature,

Table 1
Test engine specifications.

Characteristics	Specifications
Engine Type	MPFI, DOHC, Petrol
Displacement	~1000 cc
No. of Strokes	4
No. of Cylinders	3
Compression Ratio	11:1
Firing Order	1–3-2
Valvetrain	4 valves/cylinder
Cooling	Water Cooled
Aspiration	Naturally Aspirated

exhaust gas temperature before and after the TWC, intake manifold pressure, exhaust back pressure etc. The schematic of the experimental setup is shown in Fig. 1.

The fuel injection system included a fuel tank, a fuel filter and a low-pressure PFI fuel pump, which maintained a fuel injection pressure of 3.5 bar during the experiments. The fuel flow rate was calculated by measuring the time required for consumption of a specific volume of fuel. A laminar flow element (LFE) (Meriam; 50MC2-2F) was installed upstream of the air filter to measure the airflow rate to the engine by measuring the pressure drop in the manometer attached across the orifice plate of the LFE. The test engine was equipped with a stock engine control unit (ECU), which controlled the engine using factory-configured maps. Current clamps were used to obtain the ignition and fuel injection timing data at different engine test conditions. These signals were acquired by the high-speed combustion Data Acquisition System (DAQ) (AVL; Indimodule). These signals were measured along with the in-cylinder pressure w.r.t. the crank angle position to ascertain their influence on the engine-out emissions. A spark-plug based piezo-electric pressure transducer (AVL; GH13Z-24) and an optical shaft encoder (Kistler; 2614C11) were used to acquire the engine combustion data. A lambda sensor (Bosch; LSU4.9) and its display module were installed in the exhaust manifold before the TWC to obtain the lambda values during the engine operation. Emissions upstream and downstream of the TWC were measured to assess its effectiveness. The exhaust manifold and pipelines were modified to provide outlets and flow control using ball valves. Raw exhaust gas emission analyser (Horiba; MEXA-584 L) was used to measure regulated gaseous emission species in the exhaust. The measurement principles and ranges for different gaseous species measured, are given in Table 2.

A Fourier transform infrared (FTIR) emission analyser (Horiba; MEXA-6000FT-E) was used to measure traces of unregulated emission species in the engine exhaust. This analyser detected up to 32 unregulated pollutant species. Out of the 32 unregulated pollutant species, only ten were detected in measurable concentrations in the experiments and are presented in this paper. These include formaldehyde (HCHO), acetaldehyde (CH_3CHO), methanol (CH_3OH), ethanol (C_2H_5OH), methane (CH_4), ethane (C_2H_6), ethene (C_2H_4), propene (C_3H_6) and benzene (C_6H_6), and toluene (C_7H_8). The regulated and unregulated emissions were measured before and after the TWC to assess its effectiveness in controlling them, which is a novel aspect of this study. Particulate measurements were done only for engine-out emissions upstream of the TWC. An engine exhaust particle sizer (EEPS) (TSI; EEPS-3090) was used for these particulate size-number distribution measurements. EEPS measures solid particle sizes ranging from 5.6 to 560 nm with a size resolution of 16 channels per decade (a total of 32 channels). Detecting the particle size-number distributions ten times per second (10 Hz) enables transient engine measurements, if required. A rotating disc thermo-diluter (Matter Engineering; MD19-2E) was used for diluting and pre-conditioning the exhaust gas sample before passing it to the EEPS for measurements. The exhaust was preheated primarily to avoid condensation of VOCs and their entry into the thermo-diluter. The raw exhaust passes through the thermo-diluter to dilute it and maintain its temperature till it reaches the EEPS for the measurements. The dilution factor was set at 12, which resulted in a dilution of ~50 times. Pure gasoline (G100) from Indian Oil Corporation Limited (IOCL) and laboratory-grade methanol were used to prepare the test fuels for this study. Before starting the experiments, important test fuel properties, namely density and calorific value, were measured using a density-meter (Kyoto electronics; DA-130 N) and a bomb calorimeter (Parr; 6200), respectively, and the results are given in Table 3.

The engine experiments were performed at six loads and four speeds, covering the entire part-load spectrum of the engine operating envelope. The lambda values at these operating points, tuned for gasoline as per the OEM preconfigured engine map in the stock ECU, are shown in Table 4. The lambda values during M15-fueled engine experiments were targeted to achieve similar values as G100 stock ECU by controlling the
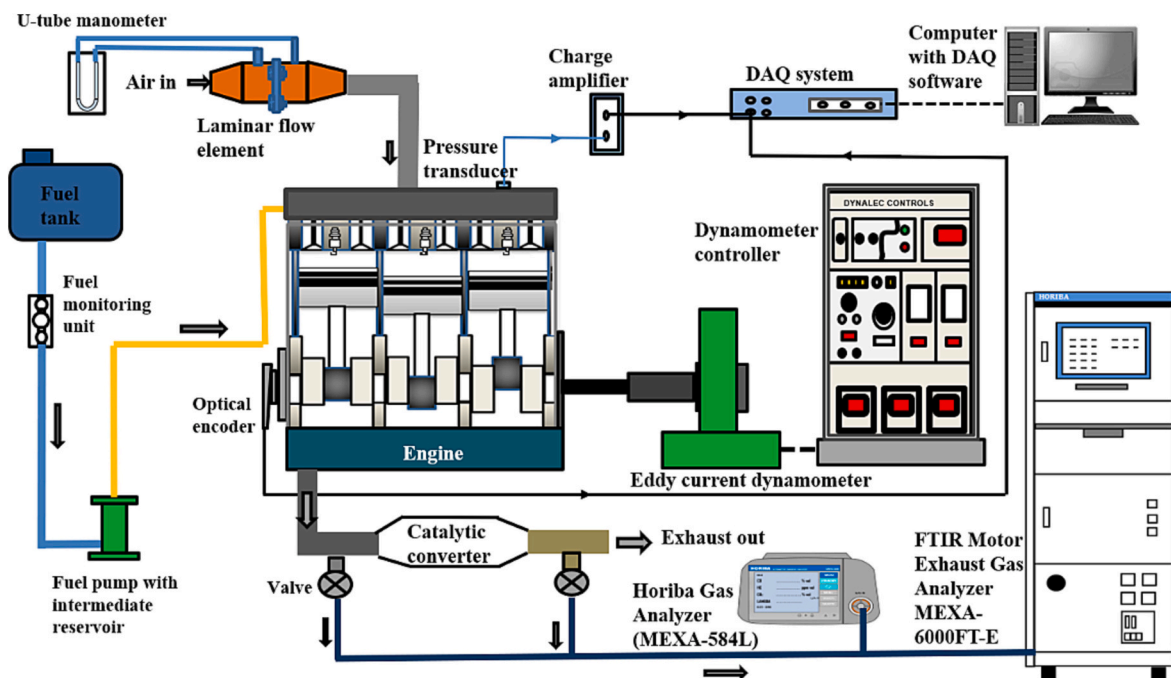
Fig. 1. Schematic of the experimental setup.

Table 2
Measurement principle and range for different gaseous species in MEXA-584 L.

Species	Measurement principle	Measurement range
CO	Non-dispersive infrared (NDIR)	0.00 to 10.00 % v/v
CO_2	Non-dispersive infrared (NDIR)	0.00 to 20.00 % v/v
HC	Non-dispersive infrared (NDIR)	0 to 10,000 ppm v/v
NO	Electrochemical sensing	0 to 5000 ppm v/v

Table 3
Tets fuel properties measured.

	G100	M15
Density (kg/m^3)	745	752
Lower Heating Value (MJ/kg)	43.9	39.3

Table 4
Target lambda values for both test fuels (Stock ECU for gasoline).

	Engine Speed (rpm)			
BMEP	1000	2000	3000	4000
1 bar	1	1	1	1
2 bar	1	1	1	1
3 bar	1	1	1	1
4 bar	1	1	1	1
5 bar	<<1	1	1	1
6 bar	<<1	1	1	<1

M15 quantity. Ignition and fuel injection timings were identical to the G100 stock ECU during the M15 testing.

2.1. Experimental uncertainty

There is always an uncertainty associated with the experimental results, which is attributed to instrumental errors, human errors, experimental procedures, improper calibration, non-repeatability of test conditions, etc. To incorporate the uncertainty associated with these factors, all the tests at a given operating condition were repeated thrice.

The average data was taken for the analysis of the results, along with standard deviations depicting the error bars. The average and standard deviations of the sample data were calculated using the following equations:

$$\text{Average, } \mu = \frac{\sum_{i=1}^{n} Xi}{n} \tag{1}$$

where X_i is the data value, and n is the number of data values.

$$\text{Standard Deviation} = \sqrt{\frac{\sum_{i=1}^{n}(Xi - \mu)^2}{n}} \tag{2}$$

3. Results and discussion

The results were analysed by measuring the regulated emission species, namely CO, HC and NOx, and unregulated emission species, such as aldehydes, alcohols, alkanes, alkenes and aromatic groups as well as the particulates. Catalytic conversion of these regulated and unregulated emission species by the TWC and its effectiveness in controlling these emissions is also investigated. The exhaust particles were assessed for particle number-size distributions and particulate mass-size distributions up to mid-load at varying engine speeds.

3.1. Regulated emissions and TWC effectiveness

Combustion of fuel-air mixture leads to the formation of several chemical species that potentially harm the human health and the environment. The government regulates such harmful species formed in significant amounts, such as HC, CO and NOx. In this section, regulated gaseous emissions, namely HC, CO and NOx, from M15 fueled engine were measured upstream and downstream of TWC to assess its effectiveness in controlling these emissions vis-à-vis baseline gasoline. The results are discussed in the following sub-sections.

3.1.1. CO emission

The combustion in the engine does not guarantee 100 % fuel conversion efficiency. The unburnt fuel fraction contributes to combustion inefficiency, resulting in the formation of unburnt hydrocarbons and CO.

When the carbon in the fuel does not oxidise to CO_2, it forms CO, which harms the human health and the environment. It triggers chemical reactions leading to ground level ozone formation and has a high greenhouse gas (GHG) index. In SI engines, the flame front engulfs the fuel-air mixture and the CO forms in fuel-rich zones due to insufficient oxygen availability. It acts as an intermediate compound formed due to high-temperature oxidation reactions of the fuel carbon, which might get converted to CO_2 upon availability of sufficient oxygen. CO formation chemistry during combustion gets frozen during the expansion of burning gases as their temperature falls. CO emission upstream and downstream of the TWC for M15 and baseline gasoline fueling of the engine at varying engine loads and speeds in the study are shown in Fig. 2.

Fig. 2 shows the engine-out CO emission upstream and downstream of the TWC. It shows that CO emission from both test fuels showed similar variations with respect to engine loads at different engine speeds. It decreased with increasing engine load, except at the highest load conditions for 1000 and 4000 rpm. Higher loads lead to high in-cylinder temperatures during combustion, favouring late oxidation of the formed CO. The CO emission significantly increased at 5 and 6 bar BMEP at 1000 rpm, mainly due to operating engine control parameters at these conditions. The ignition timings were highly retarded at these conditions to avoid knocking. Hence, the late combustion in the expansion stroke led to lower in-cylinder pressure and temperature conditions. These conditions were achieved with the richer fuel-air mixture ($\lambda < <1$)). Therefore, insufficient oxygen was available for complete combustion, increasing CO formation. Similarly, CO formed at 4000 rpm at 6 bar BMEP due to slightly richer engine operation ($\lambda < 1$). The other operating conditions were catered by a stoichiometric mixture. Compared to G100, M15 fueling decreased the engine-out CO emissions. It was ensured that the lambda matched a value similar to G100 in all engine operating conditions to observe the effect of the fuel properties of methanol. Methanol has a higher H/C ratio (4:1) than gasoline (~1.87:1), which helped reduce CO emission. The fuel oxygen in methanol also aided in the oxidation of fuel carbon. The TWC could convert the CO emission effectively for both test fuels, except at the highest load conditions at 1000 and 4000 rpm, where the engine operated on the richer side of the stoichiometry. The CO to CO_2 conversion reactions suffered for a richer fuel-air mixture due to lack of oxygen. M15 fueling showed mixed results, involving increase and decrease in the CO conversion by the TWC. However, at most operating conditions, catalytic conversion efficiency for M15 was similar or slightly higher than that of G100, as shown in Fig. 2. Hence, it can be concluded that adopting M15 in existing SI engines with TWC might be favourable from a CO emission point of view.

3.1.2. HC emissions

Another important emission species from SI engines is unburnt hydrocarbons (HC). Hydrocarbons in the exhaust form due to incomplete combustion of the fuel-air mixture in the combustion chamber. A small fraction of the charge is left unburnt, that exits the engine partially burnt and transform into HC emissions.

The in-cylinder charge occupies crevice volume during the compression stroke, which escapes combustion since the flame front cannot penetrate the narrow crevice passages. Another contribution is from the charge present around the stagnant gas layer close to the cylinder walls, where the flames extinguish, leaving this charge unburnt. The absorption of fuel hydrocarbons by the thin layer of lubricating oil on the cylinder liner is also an important HC emission source. These adsorbed fuel hydrocarbon molecules get desorbed during the expansion stroke, finding their way into the exhaust. Fig. 3 shows that HC emissions were higher at low engine speed and low load due to lower peak in-cylinder temperature, representing typical conditions susceptible to unstable combustion. HC emissions reduced upon increasing the engine load due to improved combustion stability. Although HC emission magnitudes were not much affected by the engine speed, HC emissions
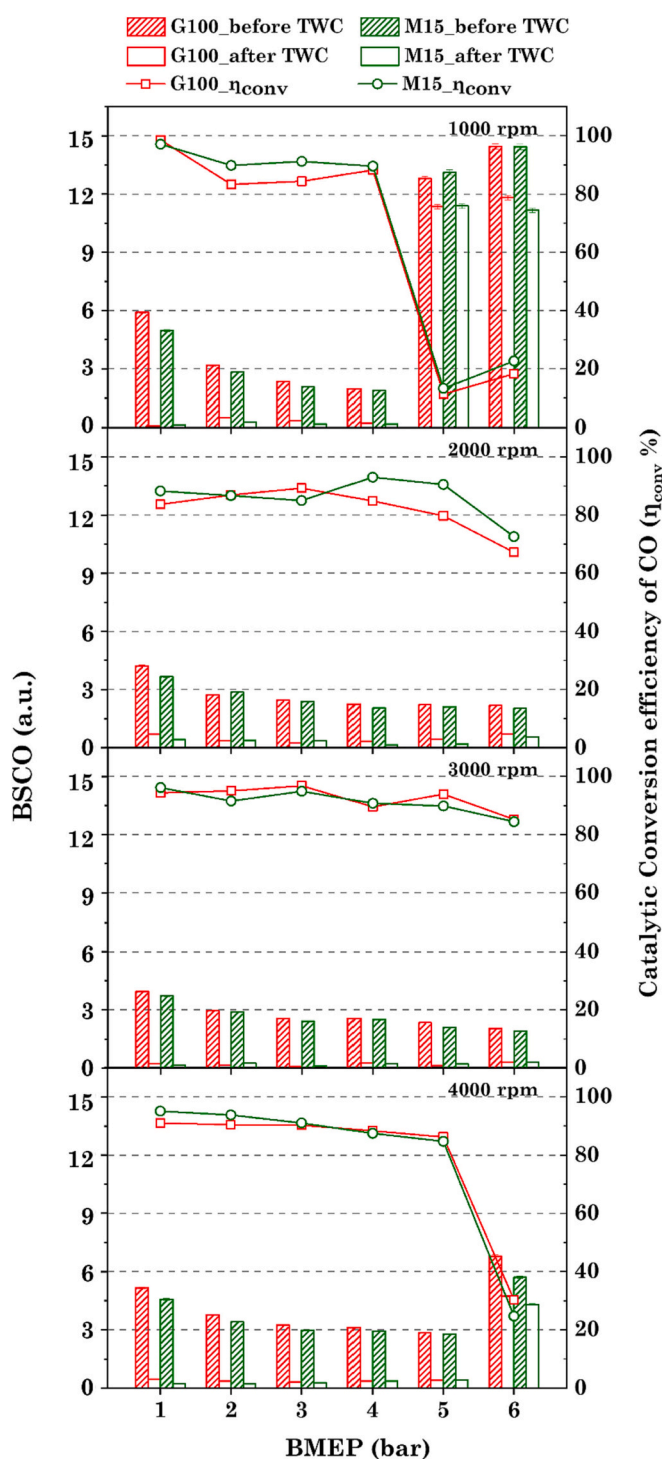

Fig. 2. CO emission upstream and downstream of the TWC and its catalytic conversion efficiency for M15 and baseline gasoline.

generally reduced with increased engine load. The mixing of hydrocarbons contributed by the quiescent charge layers and crevices with hot in-cylinder gases improved at higher engine speeds. This could have improved HC oxidation reactions in the TWC, improving its effectiveness. The replacement of G100 with M15 slightly reduced the HC emissions, which suggested that M15 fueling improved the combustion completion and HC emission oxidation processes. The higher exhaust gas temperature and lower coefficient of variation of IMEP at lower loads for M15 fueling also supported these arguments.

The fraction of partially or poorly burnt cycles also reduced due to
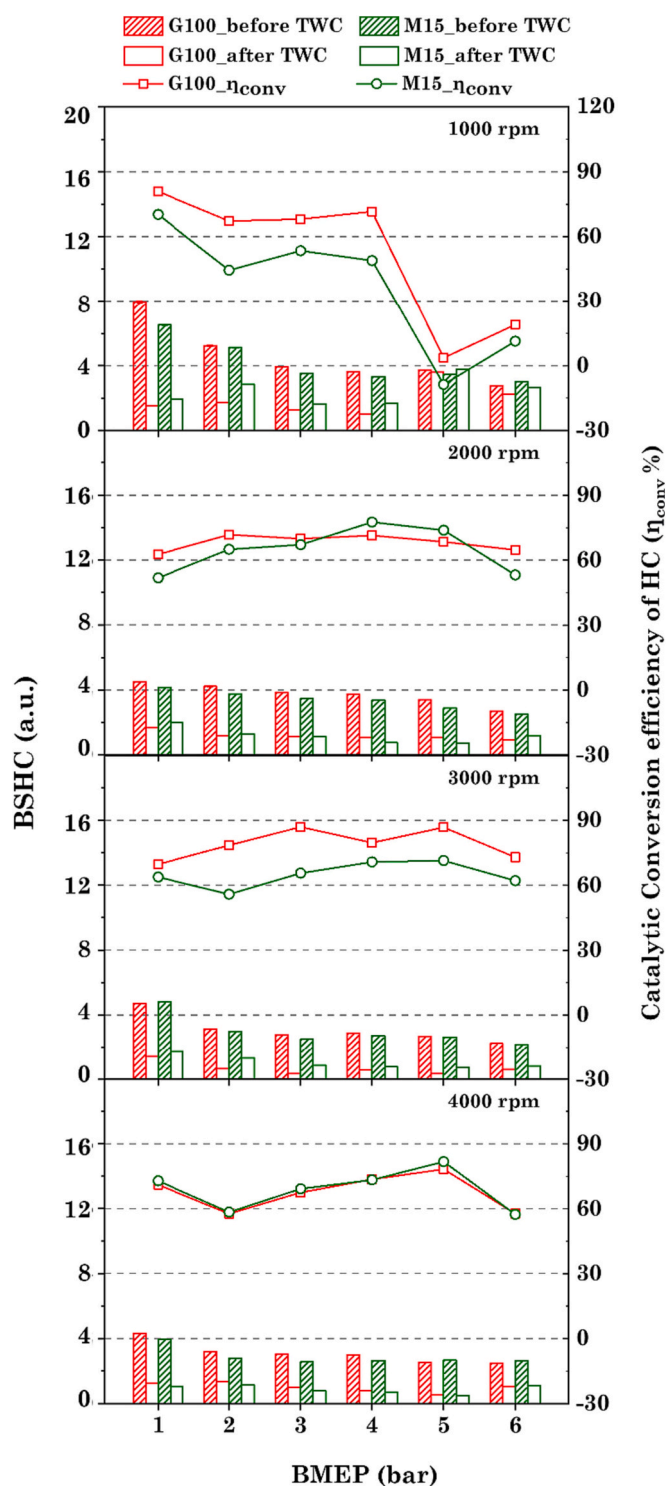
Fig. 3. HC emissions upstream and downstream of the TWC and its catalytic conversion efficiency for M15 and baseline gasoline.

higher combustion stability of M15 fueling. The fuel oxygen in M15 helped reduce carbonaceous emissions, HC and CO. However, the HC emissions downstream of TWC showed an opposite trend in Fig. 3. The catalytic conversion efficiency of HC emissions from M15 fueled engine was lower than G100 at most engine operating points. The lower catalytic conversion efficiency of M15 engine could be traced back to the composition of gases constituting hydrocarbon emissions. An increase in trace alcohol emissions for M15 downstream of TWC (Fig. 6) could be a reason for higher HC emissions than G100. At 1000 rpm, HC conversion

at 5 and 6 bar BMEP decreased due to the combustion of a richer charge, where the TWC effectiveness remained lower.

3.1.3. NOx emissions

The third important regulated emission species is 'oxides of nitrogen' (NOx). It combines NO (nitric oxide) and NO_2 (nitrogen dioxide) with a high NO/NO_2 ratio.

NOx is formed primarily due to the oxidation of nitrogen in the ambient air with oxygen in the high-temperature zones with flames and burning gases. Zeldovich reaction mechanism explains NOx formation in the engine cylinder. The engine operating conditions leading to higher peak in-cylinder pressure and temperature and stoichiometric or slightly leaner mixture conditions result in higher NOx formation. Fig. 4 shows NOx emissions upstream and downstream of the TWC, and its catalytic conversion efficiency. In general, it showed an increase with increasing engine load and speed. At 1000 rpm, NOx emissions increased upto mid-load but decreased at high loads (5 and 6 bar BMEP). This was due to combustion of richer charge at these operating points, whereas combustion was either leaner or stoichiometric at other engine operating points. Combusting richer charge reduced the peak flame temperature, and oxygen deficiency in the combustion chamber obstructed the NOx formation. In addition, the ignition timings were highly retarded (after the TDC) to avoid knocking, which reduced the peak in-cylinder pressure at these operating points. At other engine speeds, NOx emissions increased up to mid-loads and remained stable with a further increasing load.

The effect of the initial increase in engine loads was more dominant than retarded ignition timings; hence NOx emissions increased initially. Afterwards, further retarded ignition timings compensated for the effect of increased engine load. The engine at 6 bar BMEP at 4000 rpm operated slightly richer; hence NOx emissions decreased for both test fuels. M15 fueling resulted in comparable or slightly lower NOx emissions than G100, except at 5 and 6 bar BMEP at 4000 rpm. There were negligible differences in peak in-cylinder pressure. Other parameters, such as ignition timing and equivalence ratio, were maintained the same for both test fuels; hence no significant differences were observed in the NOx emissions.

Marginal differences in the NOx emissions could be traced to methanol's higher charge cooling effect during its evaporation due to its higher latent heat of vaporisation. The methanol percentage in the blend was low (15 % v/v); hence the effect of higher latent heat of methanol vaporisation was not quite prominent. Higher engine loads at 4000 rpm and higher in-cylinder temperatures due to engine operating conditions could have compensated for methanol's additional charge-cooling effect. In addition, methanol's fuel oxygen may have enhanced fuel NOx formation. The NOx emissions downstream of TWC were slightly higher for M15, indicating that NOx conversion efficiency was lower for M15 fueled engine, as shown in Fig. 4. The reduction reactions of NOx suffered in the case of M15 since the reduction reaction of formaldehyde to methanol was noticed in the TWC, as reflected in Fig. 6 in the next section.

In the TWC, a narrow air-fuel ratio window of ~0.1 near the stoichiometric air-fuel ratio (14.6) gives quite high conversion efficiencies (>80 %) for all three regulated pollutant species, namely HC, CO, and NOx. Shifting towards the richer side of this window reduces the CO and HC conversion efficiencies due to lack of oxygen, while shifting towards the leaner side decreases the NOx conversion efficiency (Heywood, 2018). These conversion reactions are highly sensitive to the air-fuel ratio. Lower catalytic conversion efficiencies of HC and CO compared to NOx were observed due to slightly richer operation closer to the stoichiometric window ($\lambda \sim 0.997$ to 0.998).

3.2. Unregulated emissions and TWC effectiveness

The government regulates harmful pollutant species formed in significant amounts, namely HC, CO and NOx. The remaining pollutant
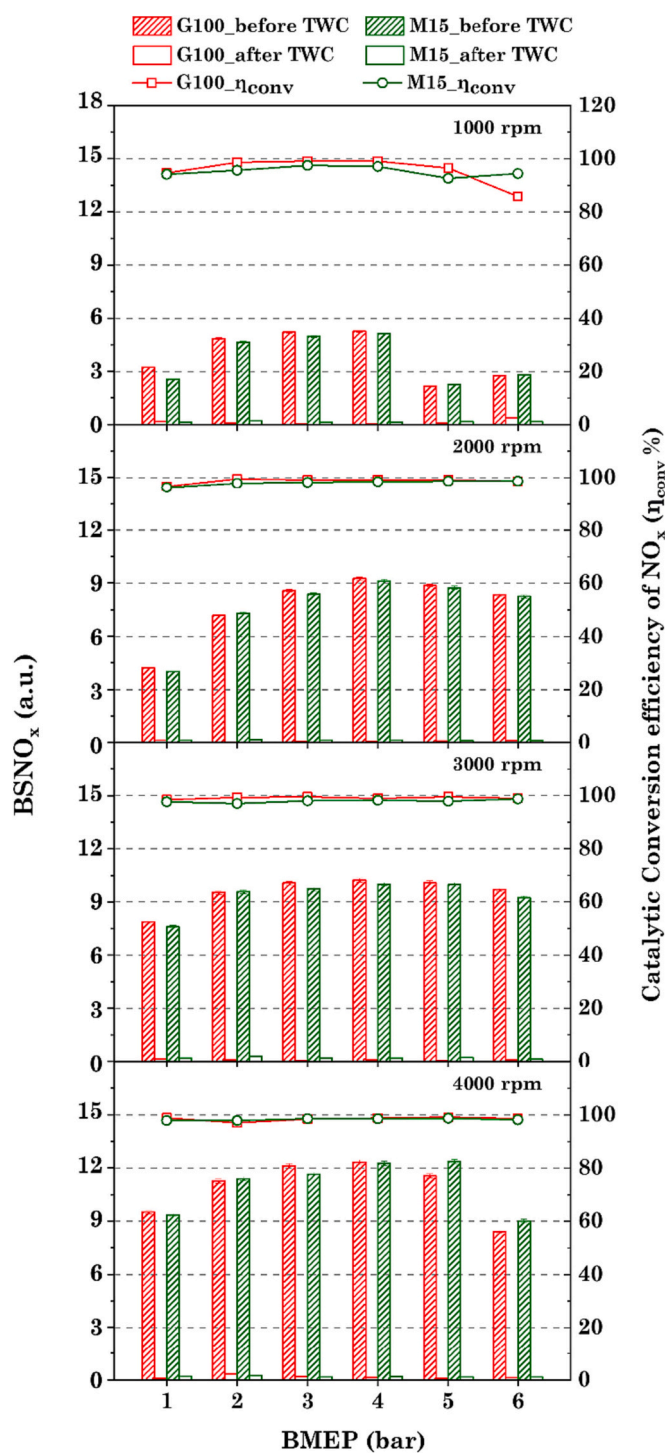
Fig. 4. NOx emissions upstream and downstream of the TWC and its catalytic conversion efficiency for M15 and baseline gasoline.

are presented in the following graphs.

Fig. 5 shows the formaldehyde (HCHO) and acetaldehyde (CH₃CHO) trace emissions from both test fuels upstream and downstream of the TWC. Aldehydes mainly form due to the oxidation of hydrocarbons in the test fuels. The primary alcohols (Methanol and Ethanol) get formed from the intermediate reactive species formed during combustion or are present in the fuel, which get further oxidised to aldehydes in the combustion chamber. HCHO and CH₃CHO are toxic species, which can cause respiratory irritation, nose bleeding and headache. The European Union (EU) and US Environmental Protection Agency (USEPA) have declared formaldehyde a potential carcinogenic and mutagenic species (Zervas et al., 2001). Fig. 5 shows that acetaldehyde emissions were higher than formaldehyde emissions, and M15 fueled engine emitted lower formaldehyde and acetaldehyde emissions than G100 fueled engine. Though higher methanol trace emissions were detected from the M15-fueled engine, formaldehyde emissions were lower than the baseline G100-fueled engine. This might be due to a higher oxidation rate of intermediate formaldehyde species formed during combustion to CO_2 in the M15-fueled engine. A few studies have also reported an opposite trend, where formaldehyde emissions increased with methanol blending of the test fuel (Ni et al., 2014; Ghadikolaei, 2016). Nevertheless, it also depends on the engine operating parameters. Lower acetaldehyde emissions from the M15-fueled engine could be traced to lower trace ethanol emissions, which upon oxidation, formed acetaldehydes. The TWC efficiencies of HCHO and CH₃CHO were generally similar for both test fuels but slightly higher for acetaldehyde.

The alcohol trace emissions assessment is essential before employing primary alcohols as fuel in the transport engines on a large-scale. Fig. 6 shows Methanol (CH₃OH) and ethanol (C₂H₅OH) trace emissions upstream and downstream of the TWC for both test fuels. Both, the combustion reactions, and the fuel contribute to these emissions.
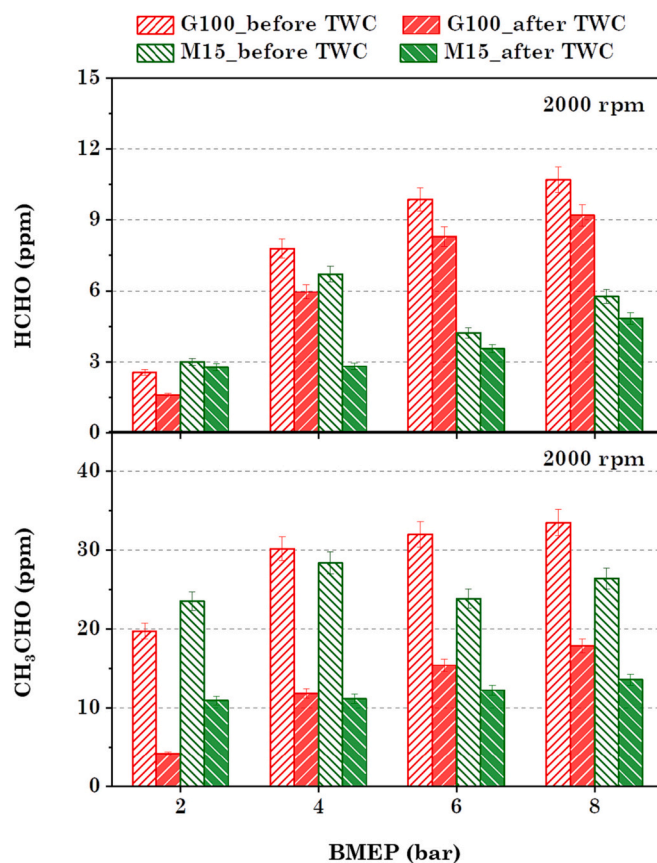

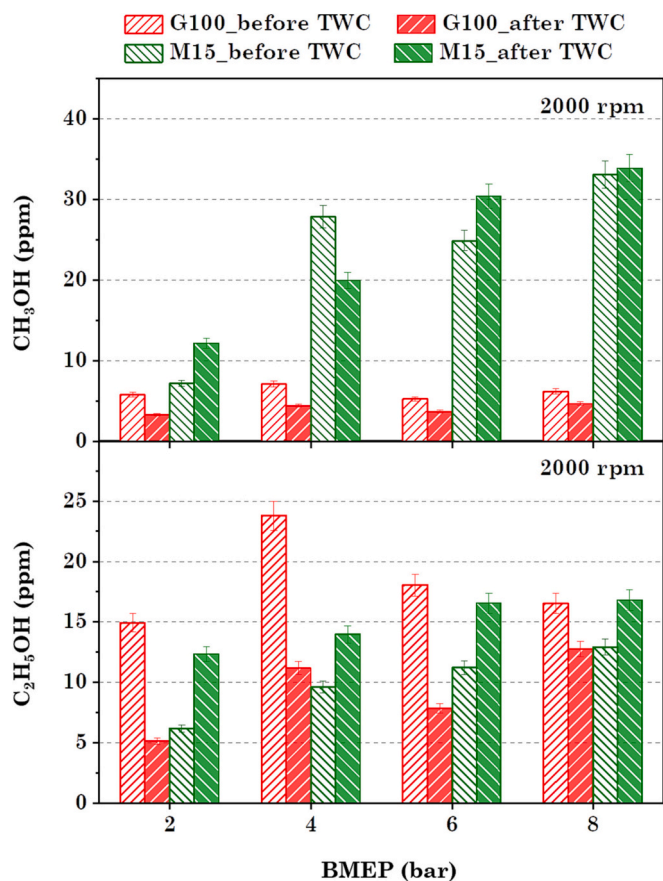**Fig. 5.** Aldehyde trace emissions upstream and downstream of the TWC for M15 and baseline gasoline.

species are termed as 'unregulated emissions,' since their emissions are in very low quantities. However, these unregulated emission species must also be investigated for all new alternative fuels being considered for large-scale implementation.

In this section, the unregulated emission species obtained in significant concentrations in the engine exhaust are presented for varying engine loads at 2000 rpm, upstream and downstream of the TWC. The unregulated emission species detected in the SI engine exhaust include aldehydes, alcohols, alkanes, alkenes and aromatics. These species are formed in the intermediate chemical reactions during combustion and

Fig. 6. Alcohol trace emissions upstream and downstream of the TWC for M15 and baseline gasoline.

Fig. 7. Alkane trace emissions upstream and downstream of the TWC for M15 and baseline gasoline.

Chemically, alcohols can form due to hydration of alkenes in presence of hydrogen ions (H^+) during combustion reactions. Exposure to fumes of primary alcohols can cause nausea, dizziness, blurred vision and headache. Fig. 6 shows that methanol trace emissions were significantly higher from the M15-fueled engine than baseline G100 fueled engine and increased with increasing engine load. These methanol and ethanol trace emissions mainly originated from the fuel. Another interesting observation is their negative TWC conversion efficiencies (net increment after the TWC) at some engine operating points. Methanol trace emissions increased downstream of TWC for M15 fueling. Because of the reduction of aldehydes, it is possible that primary alcohols are generated in the TWC when the exhaust passes through the reducing catalyst (Rh) present in the TWC.

Simpler alkanes such as methane (CH_4) and ethane (C_2H_6) are emitted by G100-fueled engines. These trace emissions form due to incomplete combustion after a series of chemical reactions leading to breakdown of complex fuel hydrocarbons into smaller and simpler hydrocarbons. However, the ethane trace concentrations were only detected only in a few ppm levels. Methane trace emissions from the engines are of concern to the environment and the human health. Methane has a high greenhouse index and is also responsible for ground-level ozone formation. When inhaled in high concentration, it can result in nausea, headache, and vomiting. Fig. 7 shows methane and ethane trace emissions from M15 and G100-fueled engines. Methane trace emissions were lower from the M15 fueled engine at all loads. Although, ethane trace emissions were higher from the M15 fueling than from the baseline G100 fueling. The TWC converter efficiency was quite similar for both test fuels. Both methane and ethane trace concentrations reduced downstream of the TWC by roughly the same order due to their catalytic oxidation.
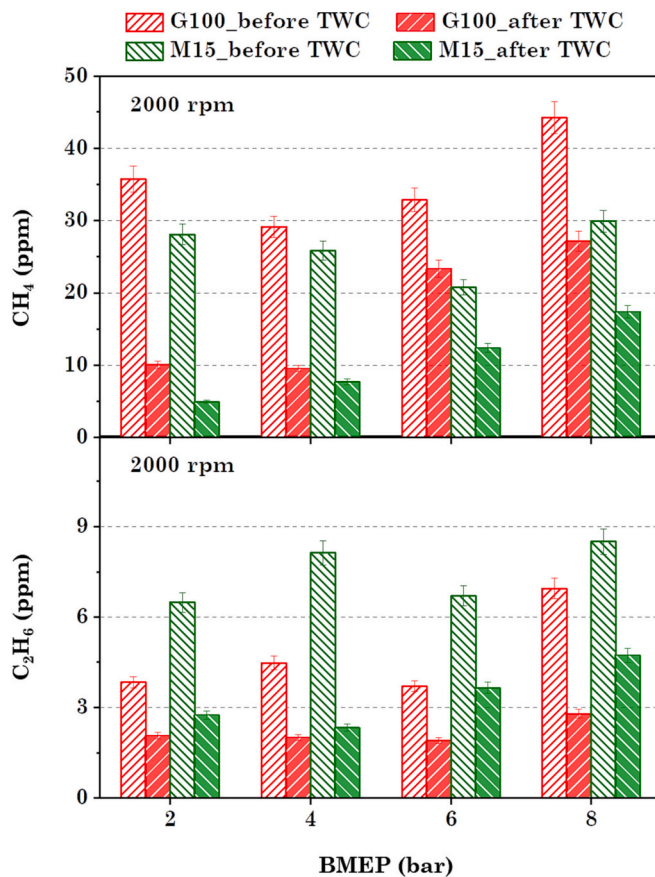
Gasoline contains molecules of different hydrocarbon families, including paraffin (alkanes), olefins (alkenes), naphthenes and aromatics. Therefore, incomplete gasoline combustion in the engine results in traces of these hydrocarbons in the exhaust. Two dominant olefins in the trace emissions detected were ethene (C_2H_4) and propene (C_3H_6). Ethene was in significantly higher trace concentrations than propene, as shown in Fig. 8. Among polycyclic aromatics compounds (PAHs), benzene (C_6H_6) and toluene (C_7H_8) traces were detected in the exhaust. Reduction of ethene to acetylene (C_2H_2) occurs due to fuel pyrolysis, which acts as a precursor to PAH formation by triggering a chain reaction, eventually leading to particulate formation. Particulates harm the human health due to their carcinogenic nature because of adsorbed PAHs on their surface.

This study demonstrated the advantages of lower trace concentrations of alkenes and PAHs in the exhaust from M15 fueled engine. The alkenes were eliminated by the TWC, while benzene and toluene were also almost eliminated by the TWC, as shown in Figs. 8 and 9. Methanol addition to gasoline reduced toluene trace concentrations upstream of the TWC, as shown in Fig. 9. The catalytic conversion efficiency of toluene was higher for M15 than for G100.

3.3. Particulate emissions

The carbonaceous soot particles form due to incomplete combustion of fuel, resulting in formation of particulate matter via a series of intermediate processes. Particulates are mainly formed by the combustion in the pockets of deficient oxygen due to a richer air-fuel mixtures, higher presence of liquid fuel droplets, or fuel films on the combustion chamber walls. Oxygen deficiency leads to fuel pyrolysis, generating intermediate by-products and radicals such as PAHs and CH^+, which are soot precursors. These soot precursors are the basis of soot nuclei
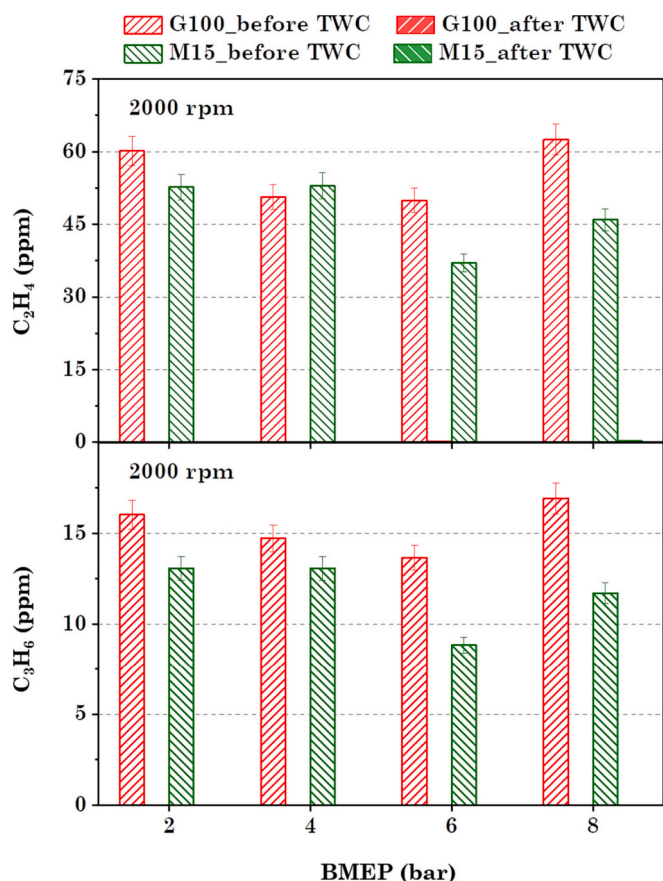
Fig. 8. Alkene trace emissions upstream and downstream of the TWC for M15 and baseline gasoline.

Fig. 9. PAH trace emission concentrations upstream and downstream of the TWC for M15 and baseline gasoline.

formation, which agglomerate, adsorb volatile organic hydrocarbons, grow and then mature into particulate matter. Along with soot formation, soot oxidation also occurs simultaneously when these soot particles move to surplus air pockets in the engine combustion chamber having high-temperature conditions. However, the time available for the oxidation of soot particles already formed is very small since the expansion stroke leads to a sharp reduction in the in-cylinder temperature, freezing the soot chemistry. The kinetics of soot formation and soot oxidation processes determine the presence of soot particles in the engine exhaust (Heywood, 2018). These particles are of different sizes of the order of nanometers up to 1 μm. Hence, they are dangerous when inhaled because of their very high surface area per unit volume/mass. These nanoparticles can penetrate deeper into the lungs and cause respiratory diseases. PAHs adsorbed on the particulate surface can lead to cancer.

Fig. 10 shows the particulate number (PN) vs size distribution for G100 and M15 fueled engines at varying engine loads and speeds. The particles smaller than 10 nm are termed as nanoparticles (NP), particles in-between 10 and 50 nm are termed as nucleation-mode particles (NMP) and particles larger than 50 nm are termed as accumulation-mode particles (AMP). The PN distribution generally follows a unimodal trend, peaking in the NMP range (20–40 nm) with a concentration of ~#10^8 particles/cm^3 of exhaust for both the test fuels. However, at some operating conditions, another smaller peak was observed for ~100 nm particles. Gasoline engines generally produce higher numbers of NMP than comparable diesel engines, which emit AMP dominantly. This is due to predominantly premixed combustion in SI engines, while CI engines undergo predominantly diffusion combustion. At an engine speed of 1000 rpm, G100 and M15 follow a similar trend of NP and NMP with a slightly lower concentration in M15 at all loads. However, an
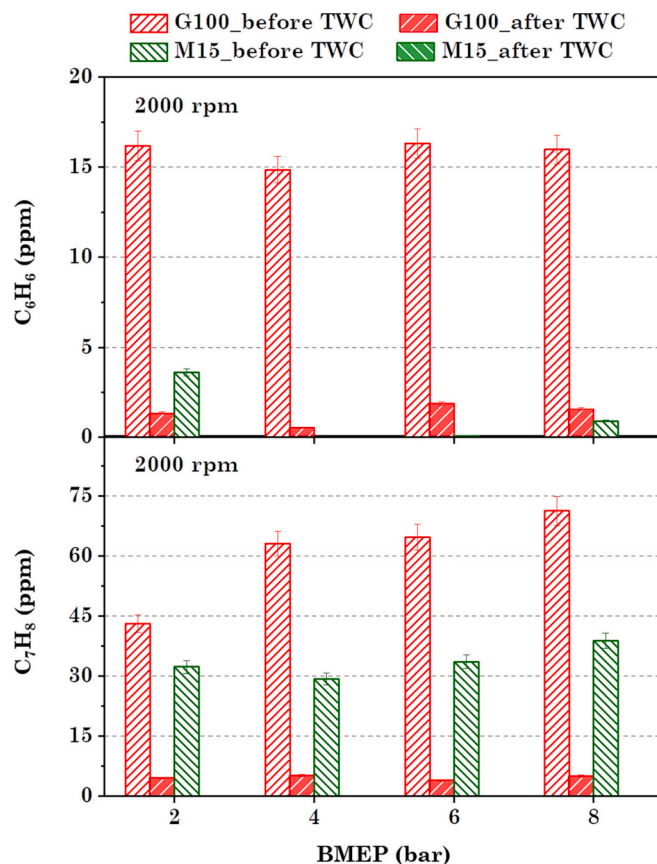
increase in PN was observed for the M15-fueled engine in the 50–100 nm particle size range. The higher AMP in M15 fueling could be because of the incomplete evaporation of larger fuel droplets in the M15 spray. Studies have showed inferior spray atomisation and fuel droplet evaporation characteristics for methanol-gasoline blends than baseline gasoline due to methanol's higher surface tension and lower volatility (Sonawane et al., 2020; Kalwar et al., 2021). Hence, liquid fuel content in the combustion chamber might be higher in the case of M15. The in-cylinder turbulence was also lower at 1000 rpm engine speed, which deteriorates the fuel-air mixing. At 2000 and 3000 rpm engine speeds, the NPs and NMPs were lower for M15. Methanol's fuel oxygen content may have supported localised soot oxidation during post-combustion reactions. Also, the formation of PAHs such as benzene and toluene, which are soot precursors, is lower in the M15-fueled engines. AMP from M15 decreased at a higher engine speed than 1000 rpm due to improved fuel-air mixing, however, it remained higher than G100. At 4000 rpm, a considerable change in PN distribution was observed over the scenario at lower engine speeds in case of G100. NP decreased, the peak of NMP increased, and an additional peak for AMP in the range of ~70–110 nm size was also observed.

On the contrary, the PN distribution from M15 was not affected much at 4000 rpm. Hence, the overall PN distribution was lower for M15 than for G100 at all engine loads at 4000 rpm. The overall time in ms for combustion and expansion would be the shortest at 4000 rpm, the highest engine speed in this study. It might not be adequate for effectively oxidising the soot particles formed by G100. Whereas for M15, the kinetics of post-combustion reactions was effective even in a shorter time scale. This could be possibly due to 50 % (w/w) oxygen present in methanol.

Fig. 11 shows the total particulate number (TPN) as the sum of NP, NMP and AMP for G100 and M15 fueled engines. TPN for G100 was
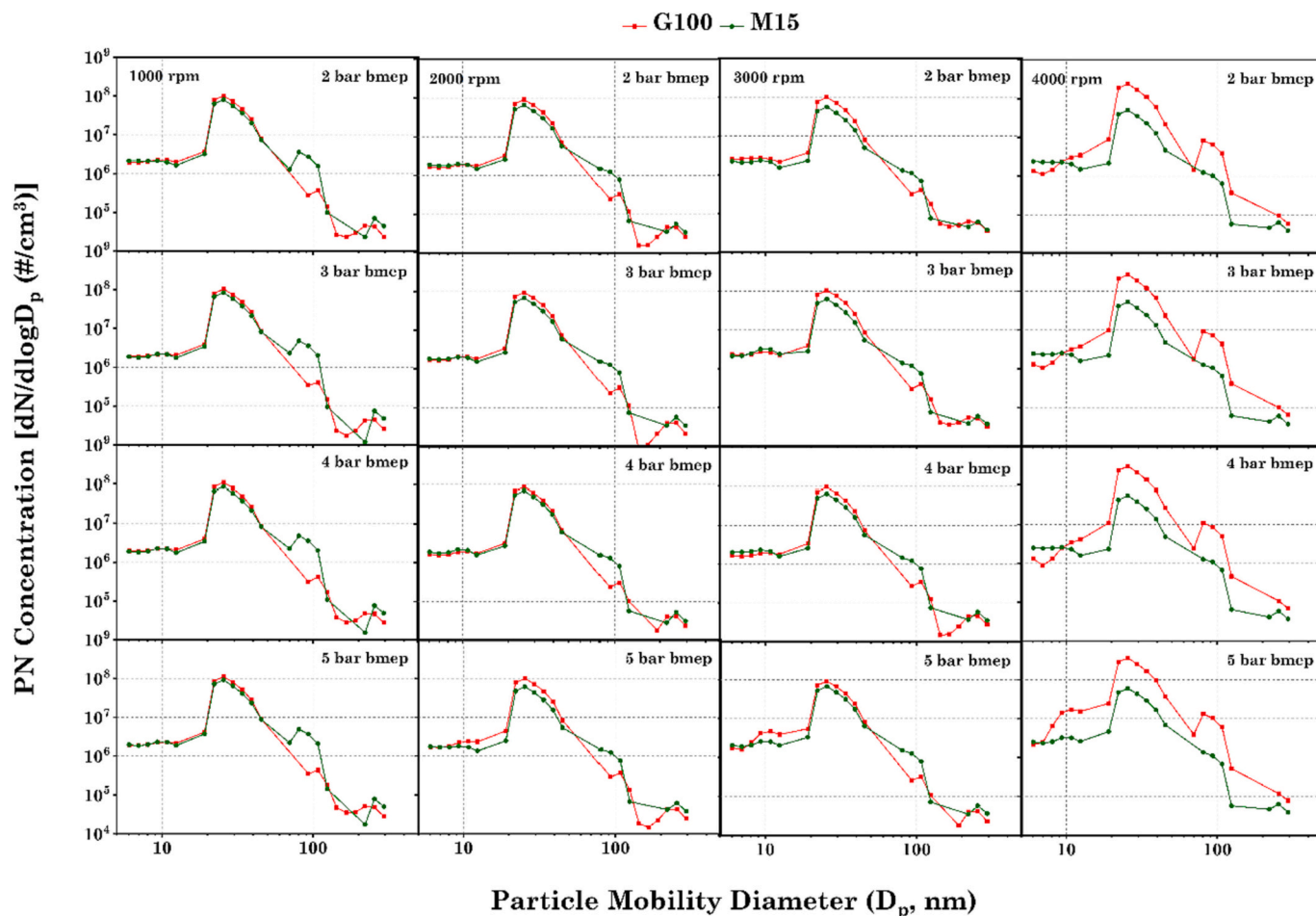
Fig. 10. PN-size distribution for M15 and baseline gasoline fueled engine.
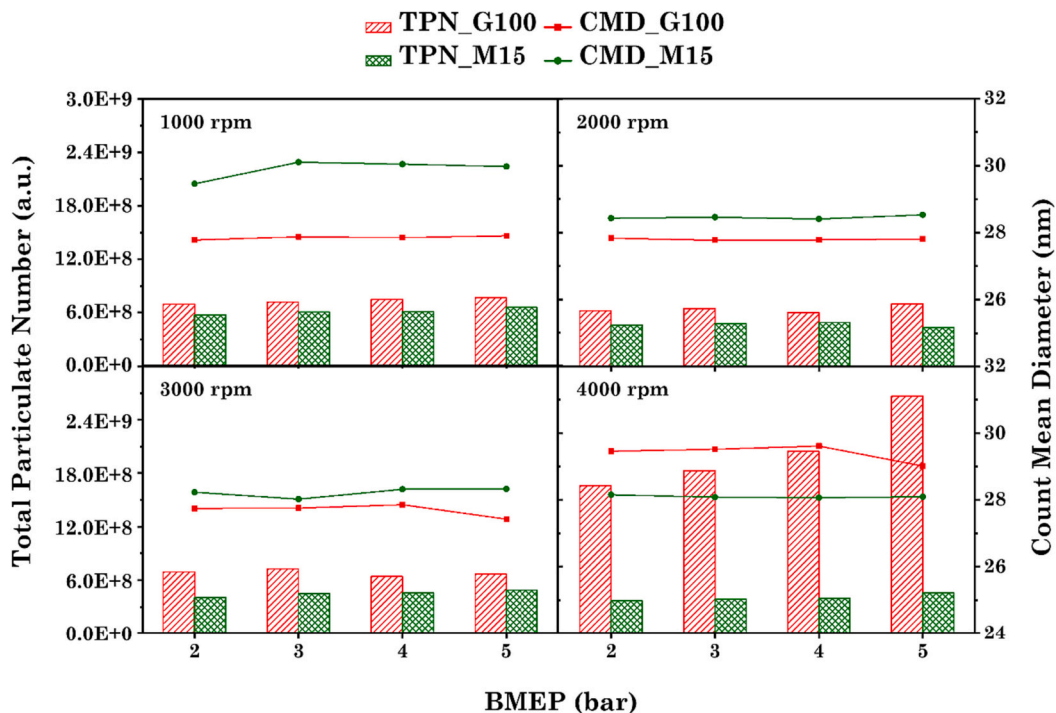

Fig. 11. TPN and CMD variations for M15 and baseline gasoline fueled engine.

observed to be of the same order at 1000, 2000 and 3000 rpm engine speeds but significantly higher at 4000 rpm. It was affected by the engine load only at 4000 rpm. As discussed previously, the soot-oxidation reaction kinetics might have been hindered due to the shorter time available. Hence, the effect of engine load was also assessed since the fuel mass combusted in the engine increased. For M15, TPN was almost similar at all engine speeds and loads. It decreased slightly at higher engine speeds and loads, though. Overall, M15 fueling showed a significant advantage of lower TPN emissions than G100, specifically at higher engine speeds. To assess the average particle size, the count mean diameter (CMD) of particulates is shown in Fig. 11. It was calculated by dividing the sum of the product of the number of particles with their corresponding size by the total number of particles. Despite lower TPN from M15, CMD was higher than G100 at the three lower engine speeds. This showed that the average particle size was higher in the M15 fueled engine exhaust. As observed in the PN distribution graph (Fig. 10), there were a higher number of AMP and a lower number of NMP emitted by M15 fueled engine, which increased the CMD of exhaust particles. However, at 4000 rpm, the CMD for G100 was higher due to an overall higher number concentration of particles of all sizes.

From the data of PN and their sizes, total particulate mass (TPM) was calculated. The calculations of TPM were based on the multiplication of the total volume of particulates of different sizes with their density. It involves an assumption that a spherical particle has a density of 1 g/cm^3, which doesn't change with particle size variations. Larger particles strongly influence the TPM. At all three engine speeds (1000, 2000 and 3000 rpm), TPM was higher for M15, as shown in Fig. 12. This could be mainly due to the emission of higher AMP from M15-fueled engines. However, at 4000 rpm, TPM for G100 increased due to higher PN for both, the NMP and the AMP.

4. Conclusions

This study experimentally explored the regulated, unregulated and particulate emission characteristics of an M15 fueled BS-VI light-duty SI engine and compared them with baseline gasoline in a factory-fitted engine configuration. The experiments were conducted at six engine loads at four engine speeds, covering the entire part-load engine operating envelope. The target lambda values were maintained constant as per factory maps (tuned for gasoline) for both test fuels by changing the fueling manually during the experiments for assessment of the effect of fuel composition alone. The other engine control parameters, namely ignition and fuel injection timings, were also per the OEM configuration. Rich mixture combustion conditions of the engine led to higher CO emissions concentrations for both test fuels. CO emissions were comparable and slightly lower for the M15-fueled engine than G100 under most test conditions. The fuel oxygen of methanol improved the degree of completion of combustion by enhancing CO-to-CO$_2$ conversion. The catalytic conversion of CO was also higher for M15 than G100 at most test points. HC emissions reduced with methanol addition to gasoline. However, HC concentration was higher for M15 fueling downstream of TWC than baseline G100. An increase in alcohol trace emissions after TWC in M15 fueling could be a probable reason. No considerable effect was observed in NOx emissions, since charge cooling might not be significant due to low methanol blending fraction in gasoline.

The catalytic conversion of NOx was lower for M15 than G100. Most unregulated emission species, namely formaldehyde, methane, ethene, toluene, and benzene, were in lower trace concentrations for M15, while Methanol and ethane trace concentrations were higher for M15 than G100. In contrast to G100, TWC showed negative conversion efficiency for trace alcohol emissions for M15 fueling. The highest conversion by TWC (~100 %) was observed for PAHs for both test fuels. In particulate emissions, PN were lower for M15 fueling. A significant reduction was observed at 4000 rpm though. PM emission was higher for M15 at lower engine speeds due to higher AMP. Methanol's combustion reaction kinetics and higher soot-oxidation rate might have shown a significant reduction in soot emissions at higher engine speeds. This study showcased the impact of a 15 % Methanol blending of gasoline on regulated, unregulated, and particulate emissions after calibration changes for maintaining identical lambda values for both test fuels. For large-scale implementation of methanol, few other aspects such as engine durability, in-service emission compliances and diagnostic functionality must be studied, along with required calibration updates.
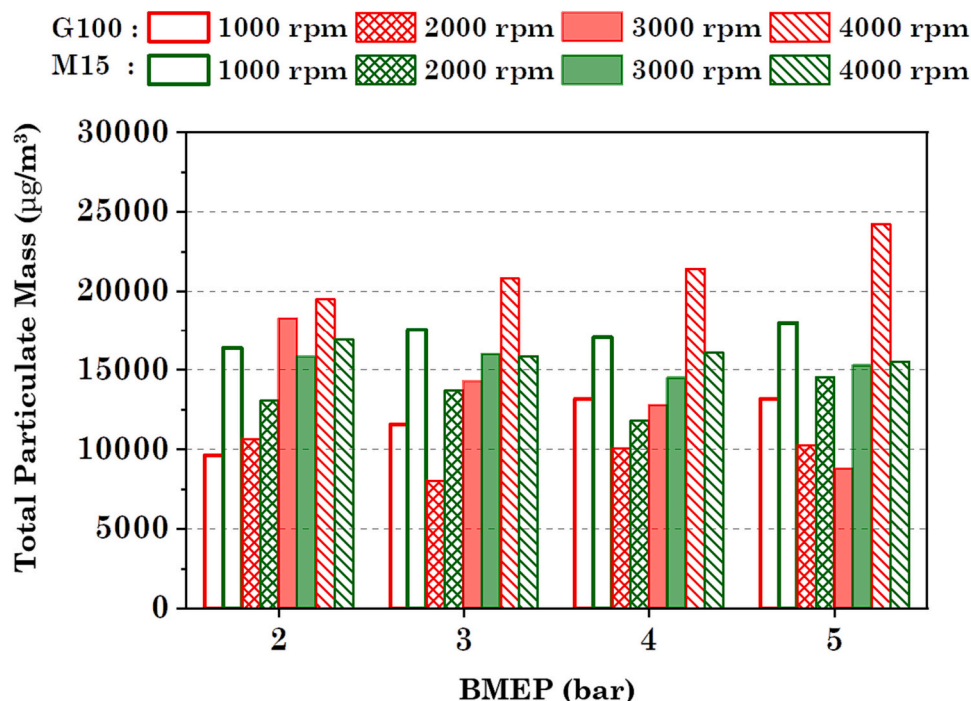

Fig. 12. TPM variations for M15 and baseline gasoline fueled engine.

CRediT authorship contribution statement

Ankur Kalwar: Conceptualization, Data curation, Formal analysis, Investigation, Writing – original draft. **Rahul Kumar Singh:** Formal analysis, Investigation. **Ankit Gupta:** Investigation. **Ranjeet Rajak:** Supervision, Writing – review & editing. **Gokul Gosakan:** Validation, Writing – review & editing. **Avinash Kumar Agarwal:** Conceptualization, Formal analysis, Methodology, Project administration, Resources, Supervision, Validation, Writing – review & editing.

Declaration of competing interest

No conflict of interest.

Data availability

The authors do not have permission to share data.

Acknowledgements

References

Agarwal, A.K., Karare, H., Dhar, A., 2014. Combustion, performance, emissions and particulate characterisation of a methanol–gasoline blend (gasohol) fuelled medium duty spark ignition transportation engine. Fuel Process. Technol. 121, 16–24.

Agarwal, A.K., Shukla, P.C., Gupta, J.G., Patel, C., Prasad, R.K., Sharma, N., 2015. Unregulated emissions from a gasohol (E5, E15, M5, and M15) fuelled spark ignition engine. Appl. Energy 154, 732–741.

Agarwal, A.K., Valera, H., Pexa, M., Čedík, J., (Eds.), 2021. Methanol: A Sustainable Transport Fuel for CI Engines. Springer Nature.

Arapatsakos, C.I., Karkanis, A.N., Sparis, P.D., 2003. Behaviour of a small four-stroke engine using as fuel methanol-gasoline mixtures. SAE Technical Paper, 2003-32-0024.

Bae, C., Kim, J., 2017. Alternative fuels for internal combustion engines. Proc. Combust. Inst. 36 (3), 3389–3413.

Balki, M.K., Temur, M., Erdoğan, S., Sarıkaya, M., Sayin, C., 2021. The determination of the best operating parameters for a small SI engine fueled with methanol gasoline blends. Sustain. Mater. Technol. 30, e00340.

Celik, M.B., Özdalyan, B., Alkan, F., 2011. The use of pure methanol as fuel at high compression ratio in a single-cylinder gasoline engine. Fuel 90 (4), 1591–1598.

Feng, S., Hong, W., Li, X., Xie, F., Su, Y., 2020. The influence of DISI engine control parameters and M15 fuel on regulated and particulate emissions under light load. Fuel 276, 118024.

Gardiner, D., Bardon, M., Rao, V., Battista, V., 1990. Review of the cold starting performance of methanol and high methanol blends in spark ignition engines: high methanol blends. SAE Technical Paper, 902181.

Geng, P., Zhang, H., Yang, S., Yao, C., 2015a. Comparative study on measurements of formaldehyde emission of methanol/gasoline-fueled SI engine. Fuel 148, 9–15.

Geng, P., Zhang, H., Yang, S., 2015b. Experimental investigation on the combustion and particulate matter (PM) emissions from a port-fuel injection (PFI) gasoline engine fueled with methanol–ultralow sulfur gasoline blends. Fuel 145, 221–227.

Ghadikolaei, M.A., 2016. Effect of alcohol blend and fumigation on regulated and unregulated emissions of IC engines—A review. Renew. Sust. Energ. Rev. 57, 1440–1495.

Güdden, A., Pischinger, S., Geiger, J., Heuser, B., Müther, M., 2021. An experimental study on methanol as a fuel in large bore high-speed engine applications–port fuel injected spark ignited combustion. Fuel 303, 121292.

Heywood, J.B., 2018. Internal Combustion Engine Fundamentals. McGraw-Hill Education.

Hu, T., Wei, Y., Liu, S., Zhou, L., 2007. Improvement of spark-ignition (SI) engine combustion and emission during cold start, fueled with methanol/gasoline blends. Energy Fuel 21 (1), 171–175.

Ito, K., Yano, T., Nagasaka, R., 1982. Unburned methanol and formaldehyde in exhaust gases from a methanol-fueled SI engine. Bulletin of JSME 25 (210), 1938–1944.

Kalwar, A., Singh, A.P., Agarwal, A.K., 2020. Utilisation of primary alcohols in dual-fuel injection mode in a gasoline direct injection engine. Fuel 276, 118068.

Kalwar, A., Chintagunti, S., Agarwal, A.K., 2021. Gasohol sprays simulations of a multi-hole GDI injector in engine-like conditions. SAE Technical Paper, 2021-01-0549.

Liang, B., Ge, Y., Tan, J., Han, X., Gao, L., Hao, L., Ye, W., Dai, P., 2013. Comparison of PM emissions from a gasoline direct injected (GDI) vehicle and a port fuel injected (PFI) vehicle measured by electrical low-pressure impactor (ELPI) with two fuels: gasoline and M15 methanol gasoline. J. Aerosol Sci. 57, 22–31.

Liu, S., Clemente, E.R.C., Hu, T., Wei, Y., 2007. Study of spark ignition engine fueled with methanol/gasoline fuel blends. Appl. Therm. Eng. 27 (11−12), 1904–1910.

Ni, P.Y., Wang, Z., Wang, X.L., Hou, L., 2014. Regulated and unregulated emissions from a non-road small gasoline engine fueled with gasoline and methanol-gasoline blends. Energy Sources, Part A: Recovery, Utilisation, and Environmental Effects 36 (14), 1499–1506.

Prasad, B.N., Pandey, J.K., Kumar, G.N., 2020. Impact of changing compression ratio on engine characteristics of an SI engine fueled with equi-volume blend of methanol and gasoline. Energy 191, 116605.

Price, P., Stone, R., Collier, T., Davies, M., 2006. Particulate matter and hydrocarbon emissions measurements: comparing first and second generation DISI with PFI in single cylinder optical engines. SAE Technical Paper, 2006-01-1263.

Shayan, S.B., Seyedpour, S.M., Ommi, F., Moosavy, S.H., Alizadeh, M., 2011. Impact of methanol–gasoline fuel blends on the performance and exhaust emissions of a SI engine. International Journal of Automotive Engineering 1 (3), 219–227.

Singh, A.P., Kumar, D., Agarwal, A. K. (Eds.), 2021. Alternative Fuels and Advanced Combustion Techniques as Sustainable Solutions for Internal Combustion Engines (Springer Nature).

Singh, A.P., Sonawane, U., Agarwal, A.K., 2022a. Methanol/ethanol/butanol-gasoline blends use in transportation engine—part 1: combustion, emissions, and performance study. Journal of Energy Resources Technology 144 (10), 102304.

Singh, A.P., Sonawane, U., Agarwal, A.K., 2022b. Methanol/ethanol/butanol–gasoline blends use in transportation engine—part 2: composition, morphology, and characteristics of particulates. Journal of Energy Resources Technology 144 (10), 102305.

Sonawane, U., Kalwar, A., Agarwal, A.K., 2020. Microscopic and macroscopic spray characteristics of Gasohols using a port fuel injection system. SAE Technical Paper, 2020-01-0324.

Storey, J.M., Barone, T.L., Thomas, J.F., Huff, S.P., 2012. Exhaust Particle Characterisation for Lean and Stoichiometric DI Vehicles Operating on Ethanol-Gasoline Blends. In: Oak Ridge National lab. (ORNL), Oak Ridge, TN (United States). Fuels, Engines and Emissions Research Center (FEERC).

Wei, Y., Liu, S., Liu, F., Liu, J., Zhu, Z., Li, G., 2009. Formaldehyde and methanol emissions from a methanol/gasoline-fueled spark-ignition (SI) engine. Energy Fuel 23 (6), 3313–3318.

Wu, B., Wang, L., Shen, X., Yan, R., Dong, P., 2016. Comparison of lean burn characteristics of an SI engine fueled with methanol and gasoline under idle condition. Appl. Therm. Eng. 95, 264–270.

Yanju, W., Shenghua, L., Hongsong, L., Rui, Y., Jie, L., Ying, W., 2008. Effects of methanol/gasoline blends on a spark ignition engine performance and emissions. Energy Fuel 22 (2), 1254–1259.

Zervas, E., Montagne, X., Lahaye, J., 2001. C1− C5 organic acid emissions from an SI engine: influence of fuel and air/fuel equivalence ratio. Environ. Sci. Technol. 35 (13), 2746–2751.